

Detection of delay in post-monsoon agricultural burning across Punjab, India: potential drivers and consequences for air quality

Tianjia Liu^{1*}, Loretta J. Mickley^{2*}, Ritesh Gautam³, Manoj K. Singh⁴, Ruth S. DeFries⁵, and Miriam E. Marlier⁶

¹Department of Earth and Planetary Sciences, Harvard University, Cambridge, MA, 02138, USA

²John A. Paulson School of Engineering and Applied Sciences, Harvard University, Cambridge, MA, 02138, USA

³Environmental Defense Fund, Washington, D.C., 20009, USA

⁴University of Petroleum and Energy Studies, Dehradun, Uttarakhand, India

⁵Department of Ecology, Evolution, and Environmental Biology, Columbia University, New York, NY, 10027, USA

⁶RAND Corporation, Santa Monica, CA, 90401, USA

*Correspondence to: Tianjia Liu (tianjialiu@g.harvard.edu), Loretta Mickley (mickley@fas.harvard.edu)

Abstract

Since the Green Revolution in the mid-1960s, a widespread transition to a rice-wheat rotation in the Indian state of Punjab has led to steady increases in crop yield and production. After harvest of the summer monsoon rice crop, the burning of excess crop residue in Punjab from October to November allows for rapid preparation of fields for sowing of the winter wheat crop. Here we use daily satellite remote sensing data to show that the timing of peak post-monsoon fire activity in Punjab and regional aerosol optical depth (AOD) has shifted later by approximately two weeks in Punjab from 2003-2016. This shift is consistent with delays of 11-15 days in the timing of maximum greenness of the monsoon crop and smaller delays of 4-6 days in the timing of minimum greenness during the monsoon-to-winter crop transition period. The resulting compression of the harvest-to-sowing period coincides with a 42% increase in total burning and 55% increase in regional AOD. Potential drivers of these trends include agricultural intensification and a recent groundwater policy that delays sowing of the monsoon crop. The delay and amplification of burning into the late post-monsoon season suggest greater air quality degradation and public health consequences across the densely-populated Indo-Gangetic Plain.

1. Introduction

Rapid increases in mechanized harvesting in the Indo-Gangetic Plain (IGP) since the mid-1980s, together with steady increases in crop production, have led many farmers to burn the abundant residue left behind by this practice (Badarinath *et al* 2006). Such burning is a quick, cheap, and efficient method to ready the fields for the next crop. However, the smoke from post-monsoon crop residue burning, primarily during October to November, amplifies severe haze events in the region (Kaskaoutis *et al* 2014), such as that observed in early November 2016 (Cusworth *et al* 2018). Of particular concern is the observed increase in aerosol loading

associated with an upward trend in post-monsoon burned area and with a shift toward a later peak in post-monsoon fires in northwestern India (Thumaty *et al* 2015, Jethva *et al* 2018, Liu *et al* 2019, Balwinder-Singh *et al* 2019, Jethva *et al* 2019). Here we use daily satellite remote sensing data to quantify the temporal shift toward later burning in the state of Punjab, the “breadbasket” of India. Such a shift would have implications for air quality degradation, since peak burning is more likely to coincide with meteorological conditions that are favorable in amplifying persistent haze, such as weak winds, low mixing layer heights, temperature inversions, and high relative humidity (Ojha *et al* 2020).

Agricultural intensification of rice and wheat in India has led to over two-fold and three-fold increases, respectively, in crop yield since the Green Revolution in the mid-1960s. In the western IGP, the predominant rice-wheat rotation is highly productive (Kumar *et al* 2015). Punjab, an agricultural state in northwestern India, contributes more than one-fifth of rice and one-third of wheat to the central grain pool in India, and thus generates large amounts of crop residue annually. Since the mid-to-late 1980s, farmers have increasingly used mechanized harvesting methods in preference to sickle-based manual harvesting in order to reduce labor costs and save time (Badarinath *et al* 2006, Kumar *et al* 2015). The use of combine harvesters, however, leaves behind an abundance of scattered and root-bound residue that is difficult to remove and thus often burned post-harvest to prepare for timely sowing of the next crop (Kumar *et al* 2015). The burning allows for quick disposal of crop residues and shortens the harvest-to-sowing transition from the *kharif* (monsoon crop) to *rabi* (winter crop) season. A quicker transition between crops also allows for earlier sowing of wheat during post-monsoon to avoid springtime heat (Lobell *et al* 2013).

However, the burning of post-monsoon rice residue can severely degrade air quality downwind of the agricultural fires over the IGP (Badarinath *et al* 2006, Singh and Kaskaoutis 2014, Kaskaoutis *et al* 2014, Liu *et al* 2018, Cusworth *et al* 2018, Jethva *et al* 2018, Sarkar *et al* 2018). In particular, smoke from rice residue burning in October and November may account for more than half the fine particulate matter (PM_{2.5}) concentrations in the Delhi National Capital Region (Cusworth *et al* 2018), which already experiences intense urban pollution from local and other regional sources (Amann *et al* 2017). A temporal shift in fire activity to later in the year could exacerbate air quality degradation since late autumn-to-winter meteorology in the IGP favors smog formation due to weak winds, frequent temperature inversions, and a shallow boundary layer (Choudhury *et al* 2007, Saraf *et al* 2010, Liu *et al* 2018).

Observations from the Moderate Resolution Imaging Spectroradiometer (MODIS), aboard NASA’s Terra and Aqua satellites, have been extensively used to investigate fire activity, crop yields, production, and phenology, and land use change detection. However, MODIS multi-day composites (8-day, 16-day) typically analyzed are insufficient to capture and resolve rapid changes in crop phenology (Zhao *et al* 2009). Here we use daily active fire and surface reflectance data from MODIS to investigate trends in agricultural activity in Punjab. Specifically, we quantify the delays in post-monsoon agricultural fire activity and determine whether the seasonal cycle of monsoon to post-monsoon vegetation greenness reveals similar delays. We conclude with a discussion of the potential drivers of these interannual changes and an analysis of the consequences for regional air quality.

2. Data and Methods

2.1 Study region

The IGP is home to over 700 million people (appendix S1.4), many of whom rely on agricultural productivity of the densely cropped belt of northern India and parts of Pakistan, Nepal, and Bangladesh for livelihood and food security. Relative to other double-cropped states in northern India, such as Haryana, Uttar Pradesh, and Bihar, Punjab has the highest rice-wheat productivity (Kumar *et al* 2015) and is spatially more homogenous in terms of fire intensity (Figure 1a), rice-wheat yields, and topography (Azzari *et al* 2017). Here we focus on Punjab during the post-monsoon rice residue burning season (defined here as September 20 to November 30), when fields are prepared for winter wheat sowing. To a lesser degree, we examine the pre-monsoon wheat residue burning season (April 1 to May 31), when fields are prepared for monsoon rice sowing (Figure 1b).

2.2 Active fires and vegetation indices

For analysis of fire activity, we sum daily 1-km maximum Fire Radiative Power (FRP), a proxy for fire intensity, derived from MODIS/Terra and Aqua (MOD14A1/MYD14A1, Collection 6). We also compare FRP with MODIS-derived fire counts and burned area and MODIS-based fire emissions from the Global Fire Emissions Database, version 4 with small fires (GFEDv4s) (Table S1). For analysis of vegetation greenness, we use daily 500-m MODIS/Terra surface reflectance (MOD09GA, Collection 6) to derive two vegetation indices, the Normalized Difference Vegetation Index (NDVI) and Normalized Burn Ratio (NBR):

$$\text{NDVI} = \frac{\rho_2 - \rho_1}{\rho_2 + \rho_1} \quad (1)$$

$$\text{NBR} = \frac{\rho_2 - \rho_7}{\rho_2 + \rho_7} \quad (2)$$

where ρ_i is the surface reflectance of MODIS band i . The wavelength range of the bands is as follows: 620-670 nm for band 1 (red), 841-876 nm for band 2 (near infrared), and 2105-2155 nm for band 7 (shortwave infrared). These active fire and surface reflectance datasets are described in more detail in appendix S1.

2.3 Statistical analysis

We estimate linear trends with residuals bootstrapping. Unlike the linear regression t-test, which assumes that the residuals are normally distributed, bootstrapping preserves and resamples from the sample residuals distribution. To obtain a sample distribution, 1000 iterations are performed in which residuals are randomly sampled with replacement for each iteration and the dependent variable y re-fit using linear regression.

2.3.1 Characterizing the temporal progression of agricultural fires

We characterize the progression of the pre-monsoon and post-monsoon burning seasons, defined in Section 2.1, of each year in order to assess interannual temporal trends. First, let $X =$

$\{x_t \mid x_1, x_2, x_3 \dots x_n\}$ denote the daily time series of a fire metric, such as FRP, during a given burning season lasting n days. We define the pre-monsoon (April 1-May 31) and post-monsoon (September 20-November 30) burning seasons with broad windows in order to capture all possible seasonal fire activity. To derive the peak burning date, k_{peak} , we fit Gaussian density curves to X , thus smoothing potential noise in FRP due to inconsistencies in observing area caused by cloud and haze cover:

$$g(t) = \gamma \cdot e^{-0.5[(t-\mu)/\sigma]^2} \quad (3)$$

where $g(t)$ is the Gaussian function to be optimized, t is days of the burning season expressed as 1 to n total days, μ is the mean of t , σ is the standard deviation of t , and γ is an arbitrary scaling parameter. k_{peak} is the day t that corresponds to the maximum value of $g(t)$. We then use the *optim* function from the R *stats* package to minimize non-linear least squares of $g(t)$ and X and to estimate the μ , σ , and γ parameters that yield the optimal Gaussian fit. As first guesses of the three parameters for the *optim* function, we set σ to 7, γ to 1, and μ to our estimate of the midpoint of the burning season, $k_{midpoint,w}$. We estimate $k_{midpoint,w}$ using a simple weighted average approach. We weight t by x_t and take the average to obtain $k_{midpoint,w}$:

$$k_{midpoint,w} = \frac{\sum_{t=1}^n (t \times x_t)}{\sum_{t=1}^n x_t} \quad (4)$$

Following Zhang *et al* (2014), we also estimate the start, midpoint, and end of the pre-monsoon and post-monsoon burning seasons for each year. We define a sequence of partial sums, $Y = \{y_k \mid y_1, y_2, y_3 \dots y_n\}$, in which $y_k = \sum_{t=1}^k x_t$. We normalize y_k by y_n , or the sum of FRP during the entire burning season. We then approximate k_β , or the first day when normalized Y has surpassed breakpoint β :

$$k_\beta = \arg \min_k \left\{ \left(\frac{y_k}{y_n} - \beta \right) \mid \left(\frac{y_k}{y_n} - \beta \right) > 0 \right\} \quad (5)$$

As in Zhang *et al* (2014), we define arbitrary breakpoints, $\beta = 0.1, 0.5$, and 0.9 , to represent the start ($k_{\beta=0.1}$ or k_{start}), midpoint ($k_{\beta=0.5}$ or $k_{midpoint}$), and end ($k_{\beta=0.9}$ or k_{end}), respectively, of the burning season.

2.3.2 Tracking crop phenology with NDVI and NBR

NDVI is widely used to characterize the cycling in vegetation growth, land cover change, and crop productivity (Yengoh *et al* 2015, Justice *et al* 1985). NBR, while typically used in burned area and burn severity classification (Key and Benson 2006), is analogous to NDVI, which relies on the visible red reflectance instead of the shortwave infrared (SWIR) reflectance. A major advantage of NBR is that compared to visible wavelengths, SWIR wavelengths can better discriminate between vegetation and bare soil (Chen *et al* 2005, Asner and Lobell 2000) and are less susceptible to atmospheric interference from smoke aerosols and thin clouds (Roy *et al* 1999, Eva and Lambin 1998, Avery and Berlin 1992). Here we use NBR as a complement to NDVI to track crop phenology with variations in vegetation greenness.

We estimate the timing of crop maturation, or maximum greenness, during the monsoon growing season with both the daily median NDVI and NBR time series. Assuming that the seasonal progression in the crop cycle is similar across years, the timing of peak greenness in the growing season diagnoses the timing of the overall growing season. To estimate the timing of the maximum monsoon greenness with the noisy daily time series, we apply weighted cubic splines smoothing with bootstrapping on time steps within a defined window that straddles the day of monsoon peak greenness. Cubic splines smoothing stitches together piecewise third-order polynomial interpolation between “knots,” or selected experimental points, and has been used extensively for crop phenology applications (Jain *et al* 2013, Mondal *et al* 2014, 2015, Jain *et al* 2017). We apply weights to the NDVI and NBR time series using the daily fraction of “usable” pixels, or those uncontaminated by clouds or thick haze (hereafter referred to as usable fraction) in the study area. This weighting follows from our greater confidence in daily median NDVI and NBR on clearer days versus cloudier and/or hazier days. Prior to bootstrapping, we make initial guesses of the four local maxima and minima: monsoon and winter peak greenness and pre-monsoon and post-monsoon trough greenness. We use these initial guesses to center a window of 300 days. Using a smoothing parameter of 0.75, we smooth the vegetation index time series with weighted cubic splines within the defined window and estimate the bootstrapped mean timing of maximum NDVI or NBR for each year. We repeat this process to estimate the earliest date when fields are ready to sow the winter crop, or trough greenness, during the post-monsoon transition period.

2.3.3 Regional aerosol optical depth exceedances

To quantify enhancements in regional air quality degradation during the post-monsoon burning season, we use MODIS/Terra Deep Blue retrievals of aerosol optical depth (AOD) over Punjab, Haryana, Delhi, and western Uttar Pradesh (i.e., encompassing the aerosol source and downwind transport regions of the IGP) (Levy *et al* 2013; appendix S1.3). Previous studies have shown that during the post-monsoon burning season, AOD co-varies with FRP, visibility, and PM, thus indicating the level of surface air quality degradation across north India (Vadrevu *et al* 2011, Kaskaoutis *et al* 2014, Liu *et al* 2018, Cusworth *et al* 2018). In order to minimize the contribution of background AOD, we analyze regionally averaged AOD “exceedances” – that is, the daily spatial mean of AOD increments above the mean AOD $+1\sigma$ for each pixel and season across Punjab, Haryana, Delhi, and western Uttar Pradesh. We analyze these daily mean AOD exceedances within the $k_{start}(FRP)$ and $k_{end}(FRP)$ window to isolate the effect of agricultural burning. To estimate the timing of peak AOD exceedances, or $k_{peak}(AOD)$, we apply Gaussian density curve optimization to values within this window expanded by two weeks. Such expansion ensures that the optimization is not thrown off by high AOD days isolated at the beginning or end of the season.

3. Results

3.1 Trends in seasonal agricultural fire activity

The bimodal distribution of peak agricultural fire activity in both pre-monsoon and post-monsoon periods is limited to northwestern India, primarily in Punjab, as well as northern

Haryana (Figures 1, S1). Generally, 80% of post-monsoon fires in Punjab are set within an approximate three-week window (23 ± 3 days) from mid-October to early November. We estimate that the timing of peak post-monsoon fire intensity has shifted later in Punjab by 1.17 days yr^{-1} (95% CI: [0.86, 1.49]), statistically significant at the 95% confidence interval (CI), indicating that the burning of rice residue has shifted later by over two weeks from 2003-2016 (Figure 2, Table S2). The timing of the start, midpoint, and end of the post-monsoon fire has shifted by a similar magnitude of 13-17 days. These findings using MODIS FRP are corroborated by similar temporal and magnitude shifts in GFEDv4s fire emissions and MODIS fire counts and burned area (Table S3). In contrast, we generally find no consistent statistically significant delays in the pre-monsoon burning season in Punjab (Table S2).

Spatially, the post-monsoon temporal shift is larger in magnitude in districts in western Punjab than in eastern Punjab (Figure S3). Moreover, the 14-year trends in total fire intensity for each 3-day block within this window signal a shift in the peak burning period, with decreasing FRP in mid-to-late October and increasing FRP in early November (Figure 2). The magnitude of peak post-monsoon fire activity, indicated by the maximum 3-day block sums of FRP, has more than doubled over the 14-year period, an increase that may be partly attributed to some homogenization in the timing of burning across districts.

3.2 Trends in vegetation greenness from monsoon to post-monsoon

We also examine whether vegetation greenness in Punjab show similar shifts during the monsoon growing season and post-monsoon harvest-to-sowing transition period. Whereas the timing of minimum NBR and NDVI occurs after near-completion of post-monsoon burning in mid-to-late November, the temporal maximum of these vegetation indices occurs near the end of the monsoon around late August or early September (Figure 1b), indicating crop maturation. In Punjab, the timing of maximum NDVI and NBR shows an overall delay of 11-15 days, with a large, abrupt shift of 7-9 days around 2008-09 (Figure 3a-b). Concurrently, there is an evident increasing trend in maximum monsoon NBR (0.06 decade $^{-1}$, 95% CI: [0.04, 0.08]) and NDVI (0.07 decade $^{-1}$, 95% CI: [0.05, 0.09]), consistent with steady increases in annual total *kharif* rice production in Punjab of 0.13 Tg yr^{-1} (95% CI: [0.09, 0.17]) (Figures 3b, S5, Table S5). Such increases in peak NBR and NDVI also suggest greater quantities of crop residue, which may lead to amplified fire intensity and emissions. In contrast to the shift in maximum NBR and NDVI, we find a smaller delay of 4-6 days in the timing of the minimum values of these indices during post-monsoon (Figure 3c-d, Table S5), indicating that the shift in the monsoon growing season is greater than the corresponding shift in the timing of the earliest date when fields are ready for winter wheat sowing. In addition, we find that the duration from the start of the burning season to trough post-monsoon greenness has decreased by 0.71 days yr^{-1} (95% CI: [-1.02, -0.39]), providing evidence for a shortened harvest-to-sowing period (Figure S6). Taken together, our results suggest that the temporal shifts in post-monsoon burning are likely associated with later sowing and harvesting of the monsoon crop.

3.2.1 The utility of NBR as a vegetation index

We have so far considered NBR and NDVI as complementary vegetation indices. Here we further demonstrate the utility of NBR for tracking crop phenology, particularly in resolving

the troughs of the crop cycle. The weaker detrended correlations ($r = 0.23 \pm 0.39$) between the two vegetation indices during transition months between the *kharif* and *rabi* seasons (May, June, October, and November) compared to other months ($r = 0.88 \pm 0.12$) support the notion that NDVI more poorly resolves and tends to “flatten” the troughs of the double-crop cycle curve (Figure S7). Moreover, the monthly distributions of detrended $r(\text{NDVI}, \text{NBR})$ values closely follow variations in greenness in the double-crop cycle, with greater correlation during seasons of crop growth. This pattern of correlation suggests that the performance of NDVI depends on the level of greenness in-field and that NDVI values at or near-minimum greenness should be interpreted with caution. However, without further investigation, the noisiness and saturation of NDVI should not be generalized to all other vegetation indices that rely partly on visible bands, including the Enhanced Vegetation Index (EVI) and Soil-Adjusted Vegetation Index (SAVI).

3.3 Trends in post-monsoon regional aerosol optical depth

To quantify the consequences of the delays in post-monsoon agricultural fire activity for regional air quality, we assess AOD exceedances during the main burning period bounded by $k_{start}(FRP)$ and $k_{end}(FRP)$. Within this window, post-monsoon AOD exceedances have increased by 55% from 2003-2016, likely associated with the reported upward trend in fire intensity (Figure 4). Similar to the magnitude of the delay in $k_{peak}(FRP)$, the timing of the peak in AOD, $k_{peak}(AOD)$, has shifted by 0.8 days yr^{-1} (95% CI: [0.47, 1.13]), or ~ 11 days during the 14-year period. The delay and increase in post-monsoon agricultural fire activity appear to drive the coherent shifting pattern in heavy aerosol loading episodes (higher AOD exceedances), notably observed in early November after 2008, despite the variability in AOD impacted by meteorology and other pollution sources, such as fireworks during the Diwali festival. Diwali lasts several days, and its timing is highly variable from year to year (October-November), following the lunar calendar. On average, the absolute difference between the timing of Diwali and the peak post-monsoon burning date is 7 days, with a range of 1-20 days (Figure S4). While Diwali fireworks, concentrated over dense population centers, can severely exacerbate urban pollution for a few days, crop residue burning contributes to widespread regional pollution for weeks (Mukherjee *et al* 2020, Ojha *et al* 2020).

4. Discussion

4.1 Implications of delays in post-monsoon fire activity

We find that the peak fire intensity of the post-monsoon burning season in Punjab has shifted later in time by over two weeks from 2003 to 2016, with a 42% increase in overall fire intensity. This delay is gradual, likely influenced by steady increases in crop production and mechanization, which yield higher amounts of excess crop residue. We hypothesize that a shortened harvest-to-sowing turnaround time after *kharif* rice harvests has amplified this increase by making it difficult for farmers to prepare fields for timely sowing of *rabi* wheat. The optimal time to sow wheat in Punjab is late October to early November (Balwinder-Singh *et al* 2016, Liu *et al* 2019), yet co-occurring post-monsoon fires indicate that fields are often not ready at this time, particularly in recent years. Since fire is a quick and cheap method to remove the leftover residue generated by combine harvesters, farmers may have even greater incentive to burn crop

residue, especially if harvests are delayed past the optimal date to sow wheat. Consistent with this hypothesis, we find that high fire intensity days preferentially occur during the latter half of the fire season, when the optimal window for sowing is shrinking. As post-monsoon fires increase in response to mechanization and pressures to sow on time, the burning season gradually trends later, further compressing the harvest-to-sowing window and increasing fire intensity rates. As a result, winter wheat sow dates across the region will likely homogenize, collapsing around a small optimal window to mitigate crop losses from increasing temperatures from February to March (Lobell *et al* 2012).

Additionally, we estimate a 55% increase in regional AOD exceedances and ~11-day delay in the timing of peak AOD within the post-monsoon burning period from 2003-2016. Delays in the post-monsoon burning season also suggest that high fire activity periods may increasingly coincide with late-autumn/winter meteorological conditions that favor severe fog/smog and haze events across the IGP (Dey 2018). Dense fog formation peaks in winter (December to January) over the IGP (Dey 2018, Gautam and Singh 2018, Ghude *et al* 2017), but in recent years there appears to be an increasing tendency in dense fog episodes observed earlier in November, coinciding with the buildup of intense smoke associated with crop residue burning activity (Figure S8). Further analysis of the long-term trends in meteorological conditions that are conducive to fog, such as western disturbances (Gautam *et al* 2007), is prerequisite to assessing possible feedbacks between meteorology and smoke from late October to November. Aside from increasing exposure to high regional PM concentrations both locally and in urban centers downwind, crop residue burning depletes soil moisture and decreases roadside visibility (Kumar *et al* 2015, Badarinath *et al* 2006, Sidhu *et al* 2015, Sinha *et al* 2015). In spite of bans, such burning continues to persist and gain traction (Tallis *et al* 2017). New technology that simultaneously reuses crop residue as mulch cover and incorporates seeds into the bare soil has been tested as an alternative to slash-and-burn methods of managing crop residue (Sidhu *et al* 2015, Tallis *et al* 2017, Shyamsundar *et al* 2019).

4.2 Potential drivers of delays in the rice-wheat rotation

Delays in the post-monsoon burning season are consistent with such shifts in the timing of monsoon peak greenness (11-15 days) and post-monsoon trough greenness (4-6 days), though the latter is of lesser magnitude. Unlike the steady shifts seen in post-monsoon burning, an abrupt delay of roughly one week occurring around 2008-09 dominates the overall delay in the timing of monsoon peak greenness, with relatively little change thereafter. Abrupt delays of similar magnitude are also apparent in the timing of the start of the post-monsoon burning season. Here we consider whether policy changes implemented around this time may have contributed toward these abrupt shifts. In 2009, in order to counteract severe groundwater depletion driven by low monsoon rainfall and widespread agricultural intensification, the Government of Punjab enacted the "Preservation of Sub-Soil Water Act" (ordinance in 2008), which prohibits sowing rice nurseries before May 10 and transplanting the resulting rice seedlings to flooded paddies before June 10 (Ramanathan *et al* 2005, Asoka *et al* 2017, Singh 2009, Tripathi *et al* 2016). The Act delays the onset of water-intensive agricultural practices that would otherwise coincide with warm temperatures and high pre-monsoon evapotranspiration rates, which lead to excessive usage of the groundwater supply from tube wells and other

reservoirs (Humphreys *et al* 2010).

Another policy that could be related to the shift is the 2008 all-India implementation of the Mahatma Gandhi National Rural Employment Guarantee Act (MGNREGA), a measure that provides a social security net to rural workers (Reddy *et al* 2014) and may have decreased the seasonal migration of workers to Punjab and led to labor shortages there (Singh 2009). Such shortages may have delayed the sowing of rice and incentivized use of combine harvesters, which may in turn explain the increase in crop residue burning. However, the already widespread transition to mechanized harvesting in Punjab, with diminishing dependence on manual labor, suggests that MGNREGA may have had a smaller impact on the timing of harvest and burning. Finally, variations in the timing of monsoon onset and withdrawal may be partly responsible for the interannual variability in these observed shifts, such as the early monsoon onset and rice maturation in 2013, but do not appear to drive the overall one-week delay in peak monsoon greenness from the 2003-2007 to 2008-2016 time periods (Figure S9). It is important to note that here we do not establish direct causality with the groundwater policy, MGNREGA, or monsoon rainfall variability, but suggest a relationship that needs to be further explored in the field. Figure S10 summarizes the potential drivers and implications of the delay in and amplification of post-monsoon fire activity associated with double-crop cycle. Although this study focuses on Punjab, similar temporal shifts may have also occurred in adjoining states, such as Haryana, that experienced both severe groundwater depletion and increases in rice production and post-monsoon fire activity (Asoka *et al* 2017, Jethva *et al* 2019, Balwinder-Singh *et al* 2019).

5. Conclusion

In summary, we show robust, statistically significant temporal shifts of over two weeks in the timing of peak fire activity during the post-monsoon burning period in Punjab over a 14-year period from 2003-2016, and smaller delays of 11-15 days in monsoon peak greenness and 4-6 days in post-monsoon trough greenness. We estimate the timing of peak FRP and regional AOD exceedances by optimizing the Gaussian mean and the start, midpoint, and end of the burning season by using the partial sums of FRP. We further demonstrate the viability and applicability of using daily MODIS surface reflectance to characterize crop cycles and the utility of NBR as a useful complement to NDVI for quantifying these vegetation changes. We hypothesize that while the gradual delays in the post-monsoon burning season are likely linked to agricultural intensification and increasing mechanization, the abrupt delay of one week around 2008-09 seen in the monsoon crop growing season appears to coincide with the state-wide groundwater policy. The unintended consequences of these temporal shifts in the double-crop cycle may be severe. First, a shortened harvest-to-sowing period may further encourage farmers to burn crop residues in order to sow winter wheat on time. Second, the timing of peak crop residue burning may increasingly coincide with winter meteorology that favors severe smog events downwind across the IGP, where we diagnose a 55% increase in AOD exceedances, defined as the increment of AOD above the mean + 1σ , over 2003-2016. For Punjab, alternative technology that combines the co-benefits of incorporating wheat seeds with rice residue and eliminating the need to burn residue, as well as switching to less water-intensive and stubble-producing crops, may alleviate the double bind of having to conserve groundwater while reducing public health exposure to smoke from post-monsoon fires.

Data Availability

All satellite-derived data used in this study are publicly available. MODIS-derived datasets can be accessed through NASA Earthdata (<https://search.earthdata.nasa.gov/>) and Google Earth Engine (Gorelick *et al* 2017) (<https://earthengine.google.com/>). The Global Fire Emissions Database, version 4s, (GFEDv4s) and MODIS and VIIRS active fire geolocations are available from GFED (<http://www.globalfiredata.org/>), University of Maryland (<http://fuoco.geog.umd.edu/>), and NASA Fire Information for Resource Management System (FIRMS) (<https://firms.modaps.eosdis.nasa.gov/>). The analyzed data that support the findings of this study are available upon reasonable request from the authors.

Acknowledgements

We thank Marena Lin and Peter Huybers for key contributions to early versions of this work and Meghna Agarwala for helpful discussions regarding this manuscript. This work was supported by a National Science Foundation Graduate Research Fellowship awarded to T.L. (DGE1745303).

References

- Amann M, Purohit P, Bhanarkar A D, Bertok I, Borken-Kleefeld J, Cofala J, Heyes C, Kieseewetter G, Klimont Z, Liu J, Majumdar D, Nguyen B, Rafaj P, Rao P S, Sander R, Schöpp W, Srivastava A and Vardhan B H 2017 Managing future air quality in megacities: A case study for Delhi *Atmos. Environ.* **161** 99–111 Online: <https://doi.org/10.1016/j.atmosenv.2017.04.041>
- Asner G P and Lobell D B 2000 A Biogeophysical Approach for Automated SWIR Unmixing of Soils and Vegetation *Remote Sens. Environ.* **74** 99–112 Online: [https://doi.org/10.1016/S0034-4257\(00\)00126-7](https://doi.org/10.1016/S0034-4257(00)00126-7)
- Asoka A, Gleeson T, Wada Y and Mishra V 2017 Relative contribution of monsoon precipitation and pumping to changes in groundwater storage in India *Nat. Geosci.* **10** 109–17 Online: <https://doi.org/10.1038/ngeo2869>
- Avery T E and Berlin G L 1992 *Fundamentals of remote sensing and airphoto interpretation* (New York, NY: Macmillan Publishing Company)
- Azzari G, Jain M and Lobell D B 2017 Towards fine resolution global maps of crop yields: Testing multiple methods and satellites in three countries *Remote Sens. Environ.* **202** 129–41 Online: <https://doi.org/10.1016/j.rse.2017.04.014>
- Badarinath K V S, Kiran Chand T R and Krishna Prasad V 2006 Agriculture crop residue burning in the Indo-Gangetic Plains - A study using IRS-P6 AWiFS satellite data *Curr. Sci.* **91** 1085–9
- Balwinder-Singh, Humphreys E, Gaydon D S and Eberbach P L 2016 Evaluation of the effects of mulch on optimum sowing date and irrigation management of zero till wheat in central Punjab, India using APSIM *F. Crop. Res.* **197** 83–96 Online: <http://dx.doi.org/10.1016/j.fcr.2016.08.016>

This is a postprint for EarthArXiv. This manuscript has been peer-reviewed and published in Environ. Res. Lett. at <https://doi.org/10.1088/1748-9326/abcc28>.

- Balwinder-Singh, McDonald A J, Srivastava A K and Gerard B 2019 Tradeoffs between groundwater conservation and air pollution from agricultural fires in northwest India *Nat. Sustain.* **2** 580–3 Online: <https://doi.org/10.1038/s41893-019-0304-4>
- Chen D, Huang J and Jackson T J 2005 Vegetation water content estimation for corn and soybeans using spectral indices derived from MODIS near- and short-wave infrared bands *Remote Sens. Environ.* **98** 225–36 Online: <https://doi.org/10.1016/j.rse.2005.07.008>
- Choudhury S, Rajpal H, Saraf A K and Panda S 2007 Mapping and forecasting of North Indian winter fog: an application of spatial technologies *Int. J. Remote Sens.* **28** 3649–63 Online: <https://doi.org/10.1080/01431160600993470>
- Cusworth D H, Mickley L J, Sulprizio M P, Liu T, Marlier M E, DeFries R S, Guttikunda S K and Gupta P 2018 Quantifying the influence of agricultural fires in northwest India on urban air pollution in Delhi, India *Environ. Res. Lett.* **13** 044018 Online: <https://doi.org/10.1088/1748-9326/aab303>
- Dey S 2018 On the theoretical aspects of improved fog detection and prediction in India *Atmos. Res.* **202** 77–80 Online: <https://doi.org/10.1016/j.atmosres.2017.11.018>
- Eva H and Lambin E F 1998 Burnt area mapping in Central Africa using ATSR data *Int. J. Remote Sens.* **18** 3473–97 Online: <https://doi.org/10.1080/014311698213768>
- Gautam R, Hsu N C, Kafatos M and Tsay S C 2007 Influences of winter haze on fog/low cloud over the Indo-Gangetic plains *J. Geophys. Res. Atmos.* **112** 1–11
- Gautam R and Singh M K 2018 Urban Heat Island Over Delhi Punches Holes in Widespread Fog in the Indo-Gangetic Plains *Geophys. Res. Lett.* **45** 1114–1121 Online: <https://doi.org/10.1002/2017GL076794>
- Ghude S D, Bhat G S, Prabhakaran T, Jenamani R K, Chate D M, Safai P D, Karipot A K, Konwar M, Pithani P, Sinha V, Rao P S P, Dixit S A, Tiwari S, Todekar K, Varpe S, Srivastava A K, Bisht D S, Murugavel P, Ali K, Mina U, Dharua M, Jaya Rao Y, Padmakumari B, Hazra A, Nigam N, Shende U, Lal D M, Chandra B P, Mishra A K, Kumar A, Hakkim H, Pawar H, Acharja P, Kulkarni R, Subharthi C, Balaji B, Varghese M, Bera S and Rajeevan M 2017 Winter fog experiment over the Indo-Gangetic plains of India *Curr. Sci.* **112** 767–84 Online: <https://doi.org/10.18520/cs/v112/i04/767-784>
- Gorelick N, Hancher M, Dixon M, Ilyushchenko S, Thau D and Moore R 2017 Google Earth Engine: Planetary-scale geospatial analysis for everyone *Remote Sens. Environ.* **202** 18–27 Online: <https://doi.org/10.1016/j.rse.2017.06.031>
- Humphreys E, Kukal S S, Christen E W, Hira G S, Balwinder-Singh, Sudhir-Yadav and Sharma R K 2010 Halting the groundwater decline in north-west India-which crop technologies will be winners? *Adv. Agron.* **109** 155–217 Online: <https://doi.org/10.1016/B978-0-12-385040-9.00005-0>
- Jain M, Mondal P, DeFries R S, Small C and Galford G L 2013 Mapping cropping intensity of smallholder farms: A comparison of methods using multiple sensors *Remote Sens. Environ.* **134** 210–23 Online: <http://dx.doi.org/10.1016/j.rse.2013.02.029>
- Jain M, Mondal P, Galford G, Fiske G and DeFries R 2017 An Automated Approach to Map Winter Cropped Area of Smallholder Farms across Large Scales Using MODIS Imagery

This is a postprint for EarthArXiv. This manuscript has been peer-reviewed and published in *Environ. Res. Lett.* at <https://doi.org/10.1088/1748-9326/abcc28>.

Remote Sens. **9** 566 Online: <http://www.mdpi.com/2072-4292/9/6/566>

Jethva H, Chand D, Torres O, Gupta P, Lyapustin A and Patadia F 2018 Agricultural Burning and Air Quality over Northern India: A Synergistic Analysis using NASA's A-train Satellite Data and Ground Measurements *Aerosol Air Qual. Res.* **18** 1756–73 Online: <http://doi.org/10.4209/aaqr.2017.12.0583>

Jethva H, Torres O, Field R D, Lyapustin A, Gautam R and Kayetha V 2019 Connecting Crop Productivity, Residue Fires, and Air Quality over Northern India *Sci. Rep.* **9** 16594 Online: <https://doi.org/10.1038/s41598-019-52799-x>

Justice C O, Townshend J R G, Holben B N and Tucker C J 1985 Analysis of the phenology of global vegetation using meteorological satellite data *Int. J. Remote Sens.* **6** 1271–318 Online: <https://doi.org/10.1080/01431168508948281>

Kaskaoutis D G, Kumar S, Sharma D, Singh R P, Kharol S K, Sharma M, Singh A K, Singh S, Singh A and Singh D 2014 Effects of crop residue burning on aerosol properties, plume characteristics, and long-range transport over northern India *J. Geophys. Res. Atmos.* **119** 5424–44 Online: <https://doi.org/10.1002/2013JD021357>

Key C H and Benson N C 2006 *Landscape Assessment (LA)*. In: Lutes, Duncan C.; Keane, Robert E.; Caratti, John F.; Key, Carl H.; Benson, Nathan C.; Sutherland, Steve; Gangi, Larry J. 2006. *FIREMON: Fire effects monitoring and inventory system* Online: https://www.fs.fed.us/rm/pubs/rmrs_gtr164/rmrs_gtr164_13_land_assess.pdf

Kumar P, Kumar S and Joshi L 2015 *Socioeconomic and Environmental Implications of Agricultural Residue Burning: A Case Study of Punjab, India* Online: <https://doi.org/10.1007/978-81-322-2014-5>

Levy R C, Mattoo S, Munchak L A, Remer L A, Sayer A M, Patadia F and Hsu N C 2013 The Collection 6 MODIS aerosol products over land and ocean *Atmos. Meas. Tech.* **6** 2989–3034 Online: <https://doi.org/10.5194/amt-6-2989-2013>

Liu T, Marlier M E, DeFries R S, Westervelt D M, Xia K R, Fiore A M, Mickley L J, Cusworth D H and Milly G 2018 Seasonal impact of regional outdoor biomass burning on air pollution in three Indian cities: Delhi, Bengaluru, and Pune *Atmos. Environ.* **172** 83–92 Online: <https://doi.org/10.1016/j.atmosenv.2017.10.024>

Liu T, Marlier M E, Karambelas A, Jain M, Singh S, Singh M K, Gautam R and DeFries R S 2019 Missing emissions from post-monsoon agricultural fires in northwestern India: regional limitations of MODIS burned area and active fire products *Environ. Res. Commun.* **1** 011007 Online: <https://doi.org/10.1088/2515-7620/ab056c>

Lobell D B, Ortiz-Monasterio J I, Sibley A M and Sohu V S 2013 Satellite detection of earlier wheat sowing in India and implications for yield trends *Agric. Syst.* **115** 137–43 Online: <http://dx.doi.org/10.1016/j.agsy.2012.09.003>

Lobell D B, Sibley A and Ivan Ortiz-Monasterio J 2012 Extreme heat effects on wheat senescence in India *Nat. Clim. Chang.* **2** 186–9 Online: <http://dx.doi.org/10.1038/nclimate1356>

Mondal P, Jain M, DeFries R S, Galford G L and Small C 2015 Sensitivity of crop cover to climate variability: Insights from two Indian agro-ecoregions *J. Environ. Manage.* **148** 21–

This is a postprint for EarthArXiv. This manuscript has been peer-reviewed and published in Environ. Res. Lett. at <https://doi.org/10.1088/1748-9326/abcc28>.

30 Online: <http://dx.doi.org/10.1016/j.jenvman.2014.02.026>

Mondal P, Jain M, Robertson A W, Galford G L, Small C and DeFries R S 2014 Winter crop sensitivity to inter-annual climate variability in central India *Clim. Change* **126** 61–76

Mukherjee T, Vinoj V, Midya S K, Puppala S P and Adhikary B 2020 Numerical simulations of different sectoral contributions to post monsoon pollution over Delhi *Heliyon* **6** e03548
Online: <https://doi.org/10.1016/j.heliyon.2020.e03548>

Ojha N, Sharma A, Manish K, Girach I, Ansari T U, Sharma S K, Singh N, Pozzer A and Gunthe S S 2020 On the widespread enhancement in fine particulate matter across the Indo-Gangetic Plain towards winter *Sci. Rep.* **10** 5862 Online: <https://doi.org/10.1038/s41598-020-62710-8>

Ramanathan V, Chung C, Kim D, Bettge T, Buja L, Kiehl J T, Washington W M, Fu Q, Sikka D R and Wild M 2005 Atmospheric brown clouds: Impacts on South Asian climate and hydrological cycle *Proc. Natl. Acad. Sci.* **102** 5326–33 Online: <https://doi.org/10.1073/pnas.0500656102>

Reddy D N, Reddy A A and Bantilan M C S 2014 The impact of Mahatma Gandhi National Rural Employment Guarantee Act (MGNREGA) on rural labor markets and agriculture *India Rev.* **13** 251–73

Roy D P, Giglio L, Kendall J D and Justice C O 1999 Multi-temporal active-fire based burn scar detection algorithm *Int. J. Remote Sens.* **20** 1031–8 Online: <https://doi.org/10.1080/014311699213073>

Saraf A, Bora A, Das J, Rawat V, Sharma K and Jain S K 2010 Winter fog over the Indo-Gangetic Plains: Mapping and modelling using remote sensing and GIS *Nat. Hazards* **52** 199–220 Online: <https://doi.org/10.1007/s11069-010-9660-0>

Sarkar S, Singh R P and Chauhan A 2018 Crop Residue Burning in Northern India: Increasing Threat to Greater India *J. Geophys. Res. Atmos.* **123** 6920–34 Online: <https://doi.org/10.1029/2018JD028428>

Shyamsundar P, Springer N P, Tallis H, Polasky S, Jat M L, Sidhu H S, Krishnapriya P P, Skiba N, Ginn W, Ahuja V, Cummins J, Datta I, Dholakia H H, Dixon J, Gerard B, Gupta R, Hellmann J, Jadhav A, Jat H S, Keil A, Ladha J K, Lopez-Ridaura S, Nandrajog S P, Paul S, Ritter A, Sharma P C, Singh R, Singh D and Somanathan R 2019 Fields on fire: Alternatives to crop residue burning in India *Science*. **365** 536–8 Online: <https://doi.org/10.1126/science.aaw4085>

Sidhu H S, Singh M, Yadvinder S, Blackwell J, Lohan S K, Humphreys E, Jat M L, Singh V and Singh S 2015 Development and evaluation of the Turbo Happy Seeder for sowing wheat into heavy rice residues in NW India *F. Crop. Res.* **184** 201–12 Online: <https://doi.org/10.1016/j.fcr.2015.07.025>

Singh K 2009 Act to Save Groundwater in Punjab: Its Impact on Water Table, Electricity Subsidy and Environment *Agric. Econ. Res. Rev.* **22** 365–386

Singh R P and Kaskaoutis D G 2014 Crop residue burning: A threat to South Asian air quality *Eos (Washington, DC)*. **95** 333–4 Online: <https://doi.org/10.1002/2014EO370001>

This is a postprint for EarthArXiv. This manuscript has been peer-reviewed and published in Environ. Res. Lett. at <https://doi.org/10.1088/1748-9326/abcc28>.

- Sinha B, Singh Sangwan K, Maurya Y, Kumar V, Sarkar C, Chandra B P and Sinha V 2015 Assessment of crop yield losses in Punjab and Haryana using 2 years of continuous in situ ozone measurements *Atmos. Chem. Phys.* **15** 9555–76
- Tallis H, Polasky S, Shyamsundar P, Springer N, Ahuja V, Cummins J, Datta I, Dixon J, Gerard B, Ginn W, Gupta R, Jadhav A, Jat M, Keil A, Krishnapriya P, Ladha J, Nandrajog S, Paul S, Lopez Ridaura S, Ritter A, Sidhu H, Skiba N and Somanathan R 2017 *The Evergreen Revolution: Six Ways to empower India's no-burn agricultural future*
- Thumaty K C, Rodda S R, Singhal J, Gopalakrishnan R, Jha C S, Parsi G D and Dadhwal V K 2015 Spatio-temporal characterization of agriculture residue burning in Punjab and Haryana, India, using MODIS and Suomi NPP VIIRS data *Curr. Sci.* **109** 1850–5 Online: <https://doi.org/10.18520/v109/i10/1850-1855>
- Tripathi A, Mishra A K and Verma G 2016 Impact of Preservation of Subsoil Water Act on Groundwater Depletion: The Case of Punjab, India *Environ. Manage.* **58** 48–59
- Vadrevu K P, Ellicott E, Badarinath K V S and Vermote E 2011 MODIS derived fire characteristics and aerosol optical depth variations during the agricultural residue burning season, north India *Environ. Pollut.* **159** 1560–9 Online: <https://doi.org/10.1016/j.envpol.2011.03.001>
- Yengoh G T, Dent D, Olsson L, Tengberg A E and Tucker C J 2015 *Use of the Normalized Difference Vegetation Index (NDVI) to Assess Land Degradation at Multiple Scales: Current Status, Future Trends, and Practical Considerations* (Springer International Publishing)
- Zhang X, Kondragunta S and Roy D P 2014 Interannual variation in biomass burning and fire seasonality derived from geostationary satellite data across the contiguous United States from 1995 to 2011 *J. Geophys. Res. Biogeosciences* **119** 1147–62 Online: <https://doi.org/10.1002/2013JG002518>
- Zhao H, Yang Z, Di L, Li L and Zhu H 2009 Crop phenology date estimation based on NDVI derived from the reconstructed MODIS daily surface reflectance data 2009 17th *International Conference on Geoinformatics* (Fairfax, VA) pp 1–6 Online: <https://doi.org/10.1109/GEOINFORMATICS.2009.5293522>

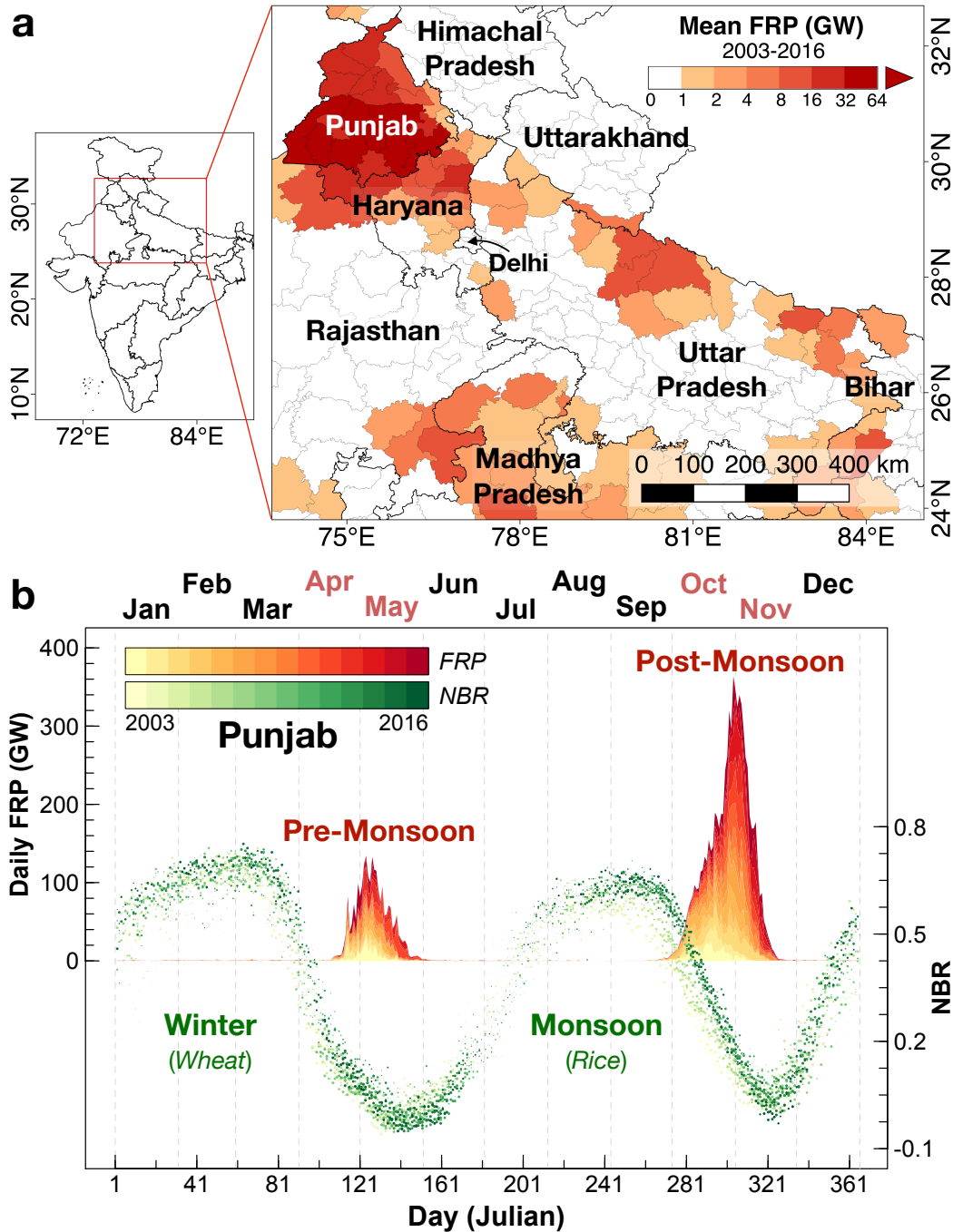


Figure 1. Cycles of fire activity and vegetation greenness in Punjab, India. District-level maps of (a) the Indo-Gangetic Plain (IGP) overlaid with annual agricultural MODIS Terra + Aqua Fire Radiative Power (GW), averaged over 2003-2016. Note that the increment of the color bar increases by a factor of 2. (b) Daily FRP (left axis) and median Normalized Burn Ratio (NBR; right axis) in Punjab. FRP values are stacked with earlier years on the bottom. The double-crop cycle indicated by NBR, a proxy for greenness, is predominantly a rice-wheat rotation. Pre-monsoon fires occur from April to May after the winter wheat growing season, and post-monsoon fires occur from October to November after the monsoon rice growing season.

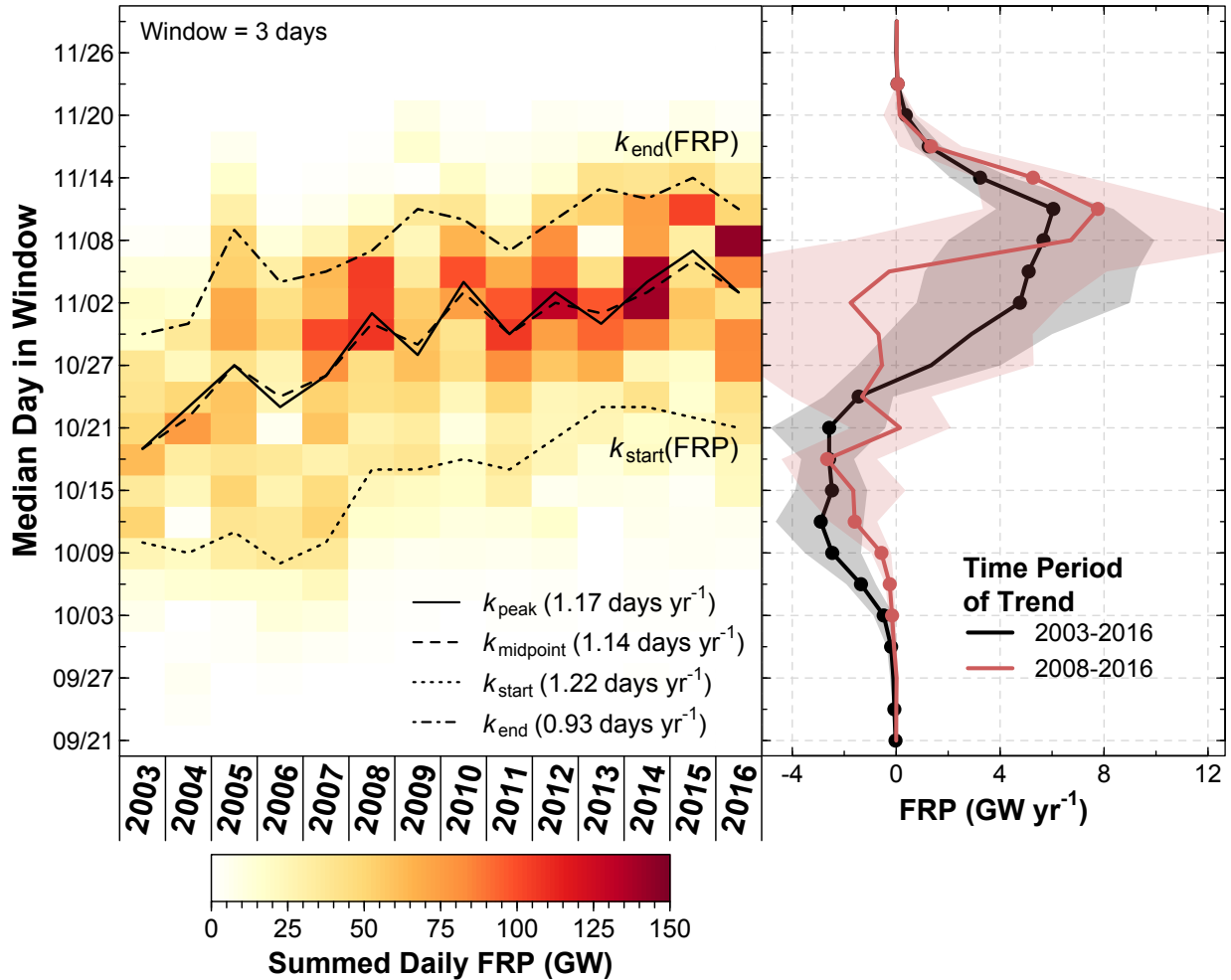


Figure 2. Temporal shifts in post-monsoon fires in Punjab from 2003-2016. (*left*) Each block represents the 3-day summed Fire Radiative Power (FRP). Dashed and solid lines represent the timing of the start, peak, midpoint, and end of the post-monsoon burning season, based on daily observations of FRP. Text inset in the left panel shows the linear trends in the $k_{start}(FRP)$, $k_{peak}(FRP)$, $k_{midpoint}(FRP)$, and $k_{end}(FRP)$; all trends shown are statistically significant at the 95% confidence level. (*right*) Trends in summed FRP (GW yr^{-1}) for each 3-day block window from September 20 to November 30 for the 2003-2016 (black line) and 2008-2016 time periods (red line). The shaded envelopes denote the 95% confidence interval, and dots represent statistically significant increases or decreases in 3-day block FRP.

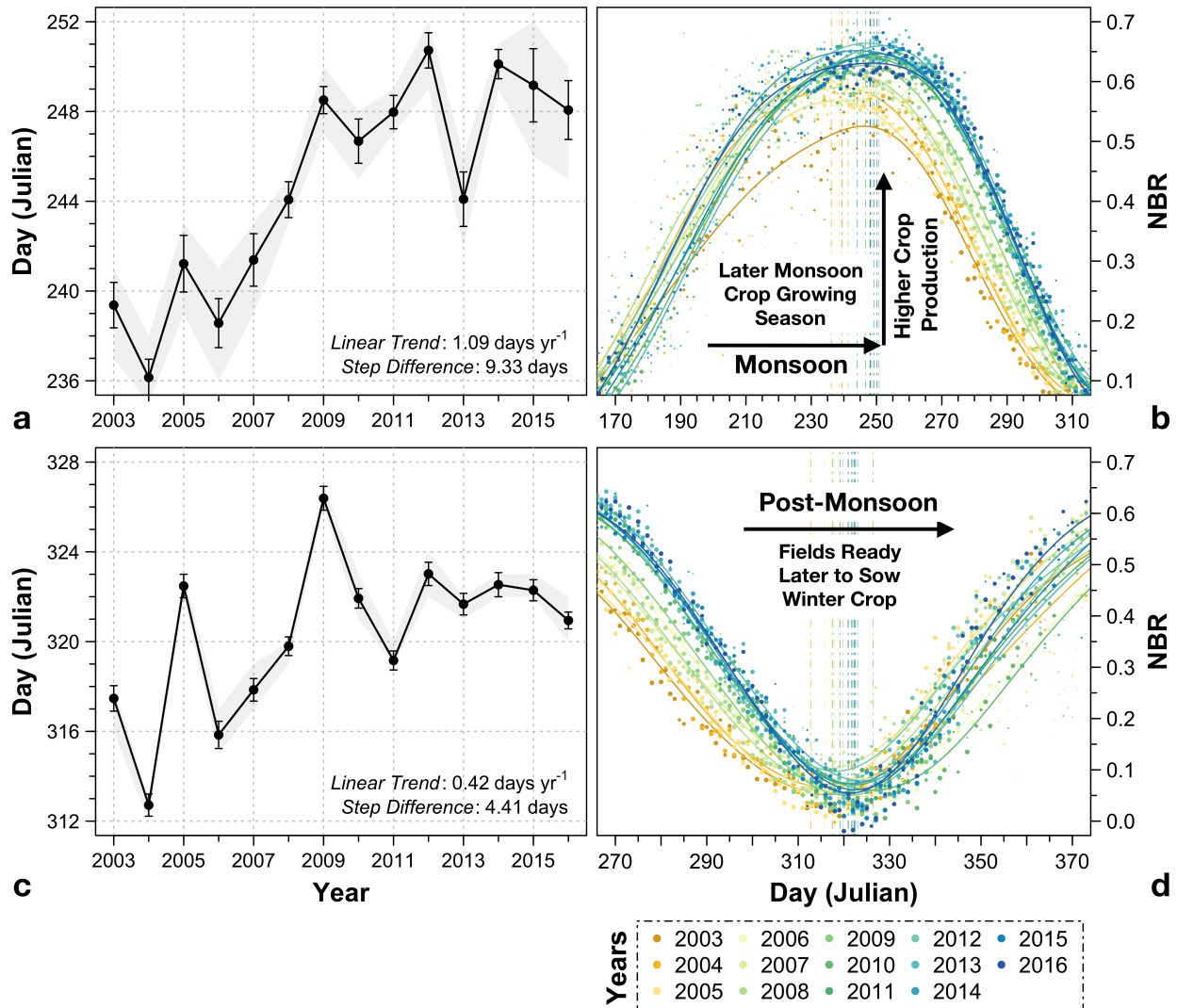


Figure 3. Trends in monsoon peak greenness and post-monsoon trough greenness in Punjab from 2003-2016. Bootstrapped mean maximum NBR during the (a) monsoon crop growing season and (c) post-monsoon harvest season, from 2003-2016. Error bars show one σ uncertainty, and shaded gray envelopes denote the 95% confidence interval. Text inset shows the bootstrapped linear trend in the timing of (a) maximum monsoon greenness and (c) minimum post-monsoon greenness from 2003-2016 and mean step difference between the 2003-2007 and 2008-2016 time periods. Daily median NBR during the (b) monsoon crop growing season and (d) post-monsoon harvest season, with lines showing the weighted parabola smoothing. Different colors denote different years. The bootstrapped mean day of (b) maximum monsoon greenness and (d) minimum post-monsoon greenness of each year is shown by vertical dashed-dot lines.

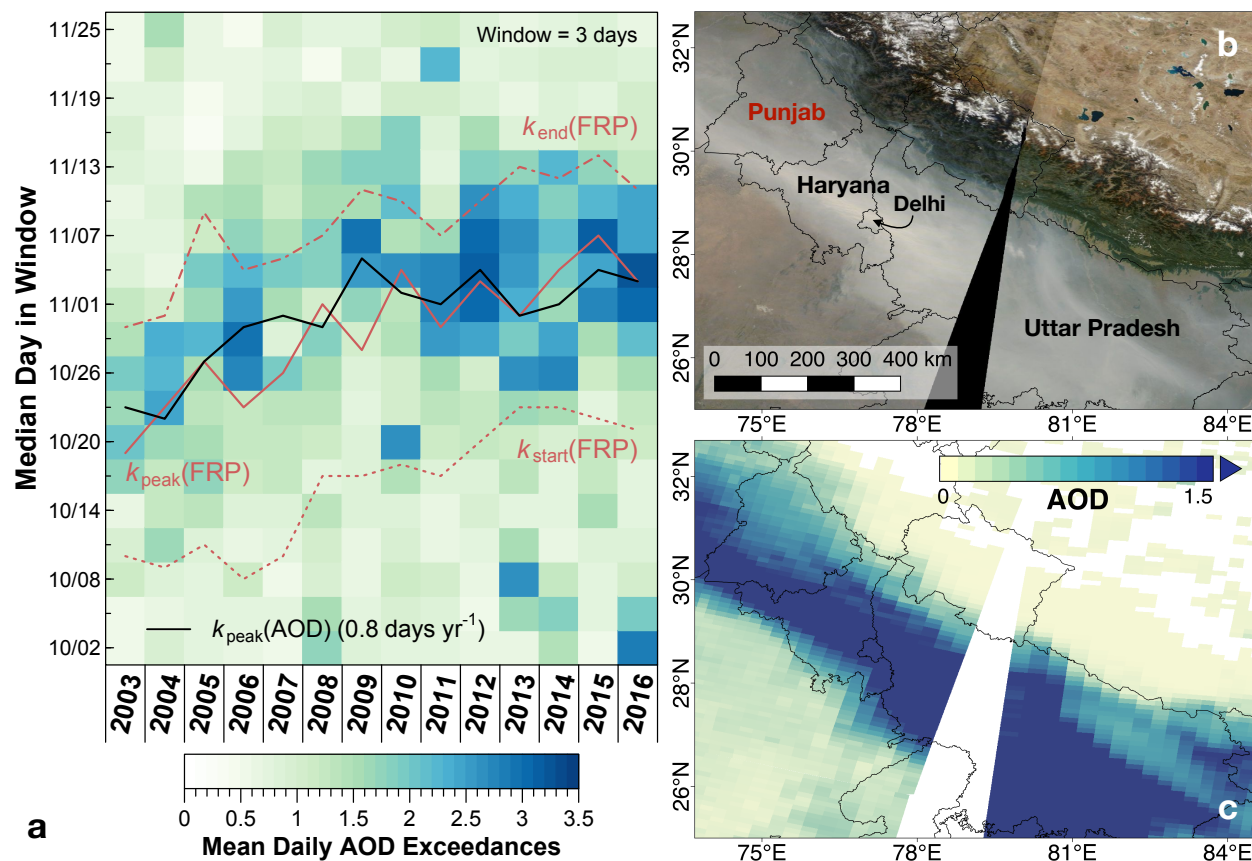


Figure 4. Trend in the timing of peak post-monsoon AOD over the western Indo-Gangetic Plain from 2003-2016. (a) Each block represents the 3-day average of regional aerosol optical depth (AOD) exceedances from the MODIS/Terra Deep Blue retrieval algorithm over Punjab, Haryana, Delhi, and western Uttar Pradesh. Here exceedances are defined as the spatially averaged AOD increments above the mean AOD + 1 σ for each season and pixel. The black line shows the timing of peak daily AOD exceedances. The red lines represent the timing of the start, peak, and end of the post-monsoon burning season, based on daily FRP (same as in Figure 2). The text inset shows the linear trend in the $k_{peak}(AOD)$, statistically significant at the 95% confidence level. Example of thick haze over the western IGP on November 6, 2016, as observed by MODIS/Terra, shown as (b) true color (NASA/Worldview; <https://worldview.earthdata.nasa.gov/>) and (c) Deep Blue AOD at 550 nm from the MOD04_L2 product.